Original Article

Corresponding Author:
Qing Wang, Institute of Mechanical Engineering and Automation College of Mechanical Engineering, Zhejiang University, 38 Zheda Road, Hangzhou 310027, China.
Email address: wqing@zju.edu.cn. Tel.: +86 13064738901.

Positioning variation modeling for aircraft panels assembly based on elastic deformation theory

Qing Wang[1,2] Renluan Hou[1,2] Jiangxiong Li[1,2] Yinglin Ke[1,2]

Paul G. Maropoulos[3] Xianzhi Zhang[4]

[1] The State Key Laboratory of Fluid Power and Mechatronic Systems, Zhejiang University, Hangzhou,310027, China

[2] Key Laboratory of Advanced Manufacturing Technology of Zhejiang Province, Zhejiang University, Hangzhou,310027, China

[3] Department of Mechanical Engineering, Aston University, Birmingham, B4 7ET, UK

[4] School of Mechanical and Automotive Engineering, Kingston University, London, SW153DW, UK

Abstract

Dimensional variation in aircraft panel assembly is one of the most critical issues that affects the aerodynamic performance of aircrafts, due to elastic deformation of parts during the positioning and clamping process. This paper proposes an assembly deformation prediction model and a variation propagation model to predict the assembly

variation of aircraft panels. An assembly deformation prediction model is derived from equations of statics of elastic beam to calculate the elastic deformation of panel component resulted from positioning error and clamping force. A variation propagation model is used to describe the relationship between local variations and overall assembly variations. Assembly variations of aircraft panels due to positioning error are obtained by solving differential equations of statics and operating spatial transformations of coordinate. The calculated results were shown to be a good prediction of variation in the experiment. The proposed method provides a better understanding of the panel assembly process and creates an analytical foundation for further work on variation control and tolerance optimization.

Keywords

aircraft panel assembly, positioning variation, elastic deformation theory, variation propagation model

Introduction

A large aircraft is commonly assembled by fuselage segments and wings, which are generally constructed by individual panels. Panel assembly is the first stage of the aircraft assembly, in which a skin has been riveted or bolted with longitudinal stiffeners (stringers) and circumferential stiffeners (frames). Each stringer-fame intersection is joined by small pieces called chips. The level of dimensional variation in panel assembly directly affects the final performance and capabilities of aircraft. However, it is difficult to predict and control the assembly variations of aircraft panels, since it is generally semimonocoque structure in large size, and the natural characteristics and assembly manners of panels often induce different degrees of deformation during assembly.

Especially in panel assembly, positioning error and clamping force of stringers and frames are of crucial effects to the dimensional variation of panels. It is necessary to develop a mathematical model of panel assembly variation to describe these effects.

The analysis of assembly variation propagation is divided into two steps. Firstly, to describe the interactions between parts and fixtures and changes between product features before and after assembly, assembly model is established for simulating assembly process. Then, individual components' variation is introduced into assembly model and the variation propagation model is adopted to estimate dimensional variation of the final product.

In the first step of variation propagation analysis approach, the assembly models have been established in several major categories in recent industrial and academic researches. A geometric model proposed by Chang and Gossard[1] is based on coordinate transformation theory, which ignores components deformation and only can be applied to rigid assembly of components with simple geometrical profile. Liu and Hu[2,3] presented a mechanical model to simplify assembly parts as 1-D cantilevered beams and derivate in-plane distortion formula of assembly joints with linear mechanics theories. A structural model proposed by Dahlstrom and Soderberg[4] is applied on early evaluation of conceptual assembly design based on a hierarchical product description and constraint

decomposition. Contrarily, Cai et al.[5] presented digital panel assembly methodologies to predict assembly dimensions with operational assembly process simulation. A virtual assembly model was utilized by Vichare et al.[6] to integrate physical in-process measurement data into wingbox assembly variation analysis with computer aided design (CAD) and finite element method (FEM) commercial software. The FEM models have been extensively utilized today as the growing complexity of assembly simulation. To raise the efficiency of FEM analysis, a construction method proposed by Lin et al.[7], used the substructures of identical parts to simplify the model, which is suitable for assembly model with numerous interchangeable parts.

After the early assembly simulation stage, the second step of assembly variations prediction is the variation propagation simulating phase. Typically, the traditional variation simulation methods include Worst Case Analysis and Root Sum of Squares which are overestimating variation spread. Subsequently, assembly variation models with considering part deformation during the assembly process are paid more attention to in analytical study. Method of Influence Coefficients (MIC) proposed by Liu and Hu[8] adopted finite element methods to construct sensitivity matrix for describing a linear relationship of input part variation and the output assembly variation. Principal Component Analysis (PCA) applied by Camelio et al.[9] extract the deformation patterns

from the production data by decomposing the component covariance into the individual contributions of several deformation patterns. Liao and Wang[10] applied wavelets transform to decompose assembly variations into different scale components and corresponding deformation of non-rigid assemblies is calculated by using FEM. For solving variation synthesis optimization problems, the statistical analysis and quality engineering methods generally aim at integrating the key production characters (KPCs) and key control characters (KCCs) to ensure the minimum assembly variation.[11] Bowman[12] utilized Monte Carlo simulation to select design tolerances for component dimensions of a mechanical assembly with minimizing manufacturing cost. Sample size exerts a big influence on the accuracy of Monte Carlo simulation. Wang[13] employed Design of Experiment (DOE) method to analyse the interactive relationship between edge's and rib's distortion. The stochastic population based on search methods is used to solve variation problems of irregular design spaces, such as simulated annealing, genetic algorithms,[14] ant colony optimization algorithms and particle swarm optimization[15]. However, it is noted that such searching methods as stochastic population cannot guarantee global optima.

Meanwhile, the focus of variation analysis of the multi-station hierarchical assembly processes is the construction of relationship between the tolerances of process

elements across multiple stages and the variation of final product. Among the models of multi-station assembly variation propagation, the State Space Method[16,17] and stream of variation methodology[18] are explored in much greater depth due to their linear structure and the automatic handling of complicated stage-wise interaction.

Most of the above proposed mathematical models utilized the linear combination of displacement of discrete KCCs to represent assembly variations of KPCs. Since non-liner behavior of the physical interaction between components and tooling is not taken into consideration in the simplified linear model, the calculated values distinctly vary from the actual assembly variations. Although FEM can simulate the nonlinear assembly process, the non-linear relationship between input dimensional variation (before assembly) and output dimensional variation (after assembly) described by FEM is implicit, which makes many non-linear analytical mathematic efforts useless.[19] In summary, it is necessary to study a nonlinear model to predict variation propagation in the assembly process. In this paper, for predicting and reducing propagation and accumulation of dimensional variation, a deformation prediction model for panel positioning assembly and a variation propagation model resulted from assembly deformation are proposed, seen in section 2. In the sections 3 and 4, the calculated results

with this method are compared with the simulation results using FEM and the measured variation data in experiments.

Deformation prediction model and variation propagation model

The assembly process of fuselage panel includes positioning, drilling, countersinking, sealing and riveting, in which the positioning accuracy of structural parts such as frames and stringers, directly affects the sequence steps. Dimension accuracy of the panel chiefly depends on the positioning accuracy of frames and stringers rather than skin because of their stronger stiffness. Meanwhile, the positioning variations of stringer will be transmitted to the next assembly stages as the stringer is fixed at the first stage. Therefore, positioning variations of stringers are investigated in the following sections.

[insert Figure 1.]

In the aircraft assembly, stringers, frames and skin shown in Fig.1 are assembled in a fixture and tacked together with temporary fasteners or fastened together with puller straps before being riveted together. The fixture is composed of fixture base, fixturing boards which are used to locate the stringers and preserve the shape of skin, and puller

straps. Clamping mechanisms fixed on the fixturing board are utilized to position and clamp the stringers, as seen in Fig.2.

[insert Figure 2.]

Deformation prediction model for stringer positioning assembly

The stringer is simplified into a beam since its cross-sectional width is much smaller than the length. When the stringer is positioned and clamped, positional variation is simplified into displacements of positioning points to clarify how variations of positioning points influence stringer deformation. Firstly, the stringer and positioning elements are simplified in panel assembly fixture to analyze positioning point variations and stringer deformation. In Fig.3, nominal position of a stringer is shown in (a), positioning point variation and stringer deformation is shown in (b).

[insert Figure 3.]

This paper adopts the energy method to calculate deformation potential of the stringer caused by variation of positioning point. Based on energy conservation theory, deformation potential is irrelevant with the sequence of forces applied on the elastomer. Instead, it is totally determined by the eventual stress and deformation. Therefore, it can be assumed that the six independent quantities of stress and their corresponding deformation components simultaneously reach the final state. An overall strain energy

density can be obtained by figuring out strain energy density of each component, and then stacking them up. The work applied on each strain is deformation potential.

[insert Figure 4.]

[insert Figure 5.]

The local coordinate system is seen in Fig. 4. Axis x_1 of the stringer is the locus of the centers of inertia of the cross-section. Axes x_2 and x_3 which are perpendicular to each other, lying in the cross-sectional plane, are shown in the Fig. 4. Displacement is $u_i = u_i(x_1), i = 1,2,3$. u_i is the displacement in x_i direction. Longitudinal displacement is u_1, lateral displacements are u_2, u_3. Since the cross area is quite small, it is assumed that the lateral displacements of the points on the same cross area are consistent, which means u_2 and u_3 are equal to deflection in two directions of x_2 and x_3 along the axis x_1, we have

$$u_2(x_1, x_2, x_3) \approx u_2^{(0)}(x_1), u_3(x_1, x_2, x_3) \approx u_3^{(0)}(x_1). \quad (1)$$

Rotation is $\omega_i = u_{3+i}, i = 1,2,3$, where ω_i is the angel rotating around axis x_i, and defined by

$$\omega_1 = u_4, \omega_2 = -\frac{du_3}{dx_1}, \omega_3 = \frac{du_2}{dx_1}. \quad (2)$$

Strain energies separately caused by tension, bending moment, torque and shear force applying on the stringer are discussed as below. For the convenience of calculation,

components of stress and corresponding directions are defined in Fig. 5.With tension applied, elongation of displacement u_1 in the direction of x_1 is positive strain, which is given by

$$\varepsilon_{11} = \varepsilon_{11}(u) = \frac{du_1}{dx_1} = u_1' . \tag{3}$$

Since stringer deformation is elastic, and based on Hooke's law, the internal force of cross section is calculated by

$$Q_1 = EA\varepsilon_{11}(u) = EAu_1' . \tag{4}$$

Strain energy occurring in the process of extension and contracting of the stringer is calculated by

$$\frac{1}{2} D_1(u,u) = \frac{1}{2}\int Q_1(u)\varepsilon_{11}(u)dx_1 = \frac{1}{2}\int EA\varepsilon_{11}^2(u)dx_1 . \tag{5}$$

With bending moment applied, curvatures around axis x_2 and x_3 are respectively given by

$$K_2 = K_2(u) = \frac{d\omega_2}{dx_1} = -\frac{d^2u_3}{dx_1^2} = -u_3'' , \tag{6}$$

$$K_3 = K_3(u) = \frac{d\omega_3}{dx_1} = \frac{d^2u_2}{dx_1^2} = u_2'' . \tag{7}$$

For the bending moment, the following equations are deduced:

$$M_2 = M_2(u) = EI_{22}K_2 + EI_{23}K_3 = -EI_{22}u_3'' + EI_{23}u_2'' , \tag{8}$$

$$M_3 = M_3(u) = EI_{32}K_2 + EI_{33}K_3 = -EI_{32}u_3'' + EI_{33}u_2'' , \tag{9}$$

where EI_{ij} is bending stiffness, I_{ij} is an inertia moment of the cross section. Furthermore, transversal shear forces generated by shear stress of σ_{21} and σ_{31} on each cross section along axis x_1 are respectively given by

$$Q_2 = Q_2(u) = -\frac{dM_3(u)}{dx_1} = -M_3{}' = EI_{32}u_3^{(3)} - EI_{33}u_2^{(3)}, \tag{10}$$

$$Q_3 = Q_3(u) = \frac{dM_2(u)}{dx_1} = M_2{}' = -EI_{22}u_3^{(3)} + EI_{23}u_2^{(3)}. \tag{11}$$

Strain energy occurring in the process of stringer bending is calculated by

$$\frac{1}{2}D_{23}(u,u) = \frac{1}{2}\int \sum_{i=2}^{3} M_i(u)K_i(u)dx_1 = \frac{1}{2}\int \sum_{i,j=2}^{3} EI_{ij}K_i(u)K_j(u)dx_1 . \tag{12}$$

With torsion applied, rate of torsion and torque are calculated from the formulae

$$K_1 = K_1(u) = \frac{d\omega_1}{dx_1} = \frac{du_4}{dx_1} = u_4{}', \tag{13}$$

$$M_1 = M_1(u) = \frac{E}{2(1+\nu)}JK_1 = GJK_1 = \frac{E}{2(1+\nu)}Ju_4{}' = \frac{E}{2(1+\nu)}J\omega_1{}', \tag{14}$$

where ν is Poisson's ratio, G is a shear elastic module, J is geometric torsional stiffness. Strain energy occurring in the process of stringer torsion is calculated by

$$\frac{1}{2}D_4(u,u) = \frac{1}{2}\int M_1(u)K_1(u)dx_1 = \frac{1}{2}\int GJK_1^2(u)dx_1 . \tag{15}$$

Thus, total strain energy is given by

$$\frac{1}{2}D(u,u) = \frac{1}{2}\left[D_1(u,u) + D_{23}(u,u) + D_4(u,u)\right]. \tag{16}$$

Virtual work functional of strain energy is expressed in terms of the components of the stress tensor in the following way

$$D_1(u,v) = \int Q_1(u)\varepsilon_{11}(v)dx_1 = \int EA\varepsilon_{11}(u)\varepsilon_{11}(v)dx_1, \tag{17}$$

$$D_{23}(u,v)=\int\sum_{i=2}^{3}M_i(u)K_i(v)dx_1=\int\sum_{i,j=2}^{3}EI_{ij}K_i(u)K_j(v)dx_1, \tag{18}$$

$$D_4(u,v)=\int M_1(u)K_1(v)dx_1=\int GJK_1(u)K_1(v)dx_1. \tag{19}$$

Total virtual work functional is given by

$$D(u,v)=D_1(u,v)+D_{23}(u,v)+D_4(u,v). \tag{20}$$

Based on the formula of integration by parts and Green's theorem, virtual work functional corresponding to the strain energy occurring in the process of extension and contracting of the stringer is written in the form

$$\begin{aligned}D_1(u,v)&=\int Q_1(u)\varepsilon_{11}(v)dx_1=\int EA\varepsilon_{11}(u)\varepsilon_{11}(v)dx_1\\&=\int EAu_1'v_1'dx_1=\left[EAu_1'v_1\right]_{\delta_1}^{\delta_2}-\int_{\delta_1}^{\delta_2}(EAu_1')'v_1dx_1,\end{aligned} \tag{21}$$

where δ_i denotes the contour of the stringer bounding the whole region.

Virtual work functional corresponding to the strain energy occurring in the process of stringer bending is extended by

$$\begin{aligned}D_{23}(u,v)&=\int\left[M_2(u)K_2(v)+M_3(u)K_3(v)\right]dx_1\\&=\int\left[-M_2(u)v_3''+M_3(u)v_2''\right]dx_1\\&=\left[M_3(u)v_2'\right]_{\delta_1}^{\delta_2}-\int_{\delta_1}^{\delta_2}M_3'(u)v_2'dx_1-\left[M_2(u)v_3'\right]_{\delta_1}^{\delta_2}+\int_{\delta_1}^{\delta_2}M_2'(u)v_3'dx_1\\&=\left[M_3(u)v_2'-M_2(u)v_3'-M_3'(u)v_2+M_2'(u)v_3\right]_{\delta_1}^{\delta_2}+\int_{\delta_1}^{\delta_2}\left[M_3''(u)v_2-M_2''(u)v_3\right]dx_1\\&=[(-EI_{32}u_3''+EI_{33}u_2'')v_2'-(-EI_{22}u_3''+EI_{23}u_2'')v_3'-(-EI_{32}u_3^{(3)}+EI_{33}u_2^{(3)})v_2\\&\quad+(-EI_{22}u_3^{(3)}+EI_{23}u_2^{(3)})v_3]_{\delta_1}^{\delta_2}+\int_{\delta_1}^{\delta_2}[(-EI_{32}u_3^{(4)}+EI_{33}u_2^{(4)})v_2-(-EI_{22}u_3^{(4)}+EI_{23}u_2^{(4)})v_3]dx_1.\end{aligned} \tag{22}$$

Virtual work functional corresponding to the strain energy occurring in the process of stringer torsion is written as

$$\begin{aligned} D_4(u,v) &= \int M_1(u)K_1(v)dx_1 \\ &= -\int_{\delta_1}^{\delta_2}\left[M_1'(u)v_4\right]dx_1 + \left[M_1(u)v_4\right]_{\delta_1}^{\delta_2}. \end{aligned} \tag{23}$$

The force that the stringer loaded can be defined as $f_i = f_i(x_1), i = 1,2,3$. f_i is the linear force along the axis x_i, then the torque load is the linear force along the axis x_i is denoted by $m_1 = m_1(x_1) = f_4(x_1)$.External work of tensile force, bending force and torsional force loaded on stringer are respectively given by

$$-F_1(v) = -\int f_1 v_1 dx_1 = -\int_{\delta_1}^{\delta_2} f_1 v_1 dx_1 = -\int_{\delta_1}^{\delta_2} f_1 v_1 dx_1 - \left[f_1 v_1\right]_{\delta_1} - \left[f_2 v_2\right]_{\delta_2}, \tag{24}$$

$$\begin{aligned} -F_{23}(v) &= -\int (f_2 v_2 + f_3 v_3)dx_1 = -\int_{\delta_1}^{\delta_2} (f_2 v_2 + f_3 v_3)dx_1 \\ &= -\int_{\delta_1}^{\delta_2} (f_2 v_2 + f_3 v_3)dx_1 - [f_2 v_2]_{\delta_1} - [f_3 v_3]_{\delta_1} - [f_2 v_2]_{\delta_2} - [f_3 v_3]_{\delta_2}, \\ &\quad -[f_5 v_5]_{\delta_1} - [f_5 v_5]_{\delta_2} - [f_6 v_6]_{\delta_1} - [f_6 v_6]_{\delta_2}, \end{aligned} \tag{25}$$

$$-F_4(v) = -\int m_1 \omega_1 dx_1 = -\int_{\delta_1}^{\delta_2} f_4 v_4 dx_1 = -\int_{\delta_1}^{\delta_2} f_4 v_4 dx_1 - \left[f_4 v_4\right]_{\delta_1} - \left[f_4 v_4\right]_{\delta_2}. \tag{26}$$

The potential energy of the system is equal to the difference between the strain energy and the work of external forces, which can be obtained by

$$J(u) = \frac{1}{2} D(u,u) - F(u). \tag{27}$$

Based on the principle of minimum potential energy of the system, the stationary value of functional $J(u)$ in the equilibrium position is a minimum, which is equivalent to $D(u,v) - F(v) = 0$ for all v, namely

$$
\begin{aligned}
D(u,v)-F(v) &= D_1(u,v)+D_{23}(u,v)+D_4(u,v)-F_1(v)-F_{23}(v)-F_4(v)\\
&= -\int_{\delta_1}^{\delta_2}[Q_1(u)+f_1]v_1dx_1+[Q_1(u)-f_1]_{\delta_2}[v_1]_{\delta_2}-[Q_1(u)+f_1]_{\delta_1}[v_1]_{\delta_1}\\
&\quad+\int_{\delta_1}^{\delta_2}[M_3''(u)-f_2]v_2dx_1-\int_{\delta_1}^{\delta_2}[M_2''(u)+f_3]v_3dx_1\\
&\quad+[M_3(u)-f_6]_{\delta_2}[v_6]_{\delta_2}+[M_2(u)-f_5]_{\delta_2}[v_5]_{\delta_2}-[M_3'(u)+f_2]_{\delta_2}[v_2]_{\delta_2}\\
&\quad+[M_2'(u)-f_3]_{\delta_2}[v_3]_{\delta_2}-[M_3(u)+f_6]_{\delta_1}[v_6]_{\delta_1}-[M_2(u)+f_5]_{\delta_1}[v_5]_{\delta_1}\\
&\quad+[M_3'(u)-f_2]_{\delta_1}[v_2]_{\delta_1}-[M_2'(u)+f_3]_{\delta_1}[v_3]_{\delta_1}\\
&\quad-\int_{\delta_1}^{\delta_2}[M_1'(u)+f_4]v_4dx_1+[M_1(u)-f_4]_{\delta_2}[v_4]_{\delta_2}-[M_1(u)+f_4]_{\delta_1}[v_4]_{\delta_1}\\
&= 0.
\end{aligned}
\tag{28}
$$

When the stringer is free from geometric constraint, based on variation principle, u in an equilibrium state makes the equation true for all v (including v_i), which is equivalent to the equilibrium equation with each factor of […] in the above equation equal to 0, all equilibrium equations are as listed below

$$
\delta_1 < x_1 < \delta_2 : -\frac{dQ_i(u)}{dx_1} = f_i \qquad i=1,2,3, \tag{29}
$$

$$
-\frac{dM_1(u)}{dx_1} = f_4, \tag{30}
$$

which is

$$
\delta_1 < x_1 < \delta_2 : \begin{cases} -EAu_1'' = f_1 \\ -EI_{32}u_3^{(4)} + EI_{33}u_2^{(4)} = f_2 \\ EI_{22}u_3^{(4)} - EI_{23}u_2^{(4)} = f_3 \\ -\dfrac{E}{2(1+\nu)}J\omega_1'' = m_1 \end{cases}, \tag{31}
$$

$$
x_1 = \delta_1 : \quad \begin{cases} -Q_i(u) = [f_i]_{\delta_1} \\ -M_i(u) = [f_{3+i}]_{\delta_1} \end{cases} \qquad i=1,2,3, \tag{32}
$$

$$
x_1 = \delta_2 : \quad \begin{cases} -Q_i(u) = [f_i]_{\delta_2} \\ -M_i(u) = [f_{3+i}]_{\delta_2} \end{cases} \qquad i=1,2,3. \tag{33}
$$

The above formulae with $x_1 = \delta_1, x_1 = \delta_2$ satisfies boundary compatibility conditions and also natural boundary condition, indicating the balance of shearing force, tension, bending moment and torque at the endpoint. When the stringer is subject to geometric constraint and any generalized displacement u_i, specified by some endpoint is known, replace equations of load f_i that have the same subscript. Imposed boundary conditions is

$$x_1 = \delta_x : \begin{cases} u_i = \bar{u}_i^{\delta_x} \\ \omega_i = \bar{\omega}_i^{\delta_x} \end{cases}, i = 1,2,3. \tag{34}$$

With simultaneous equations above, we can solve the function expression of stringer deformation $u_i(x_1)$ $(i = 1,2,3,4)$. Furthermore, the relationship of assembly variations and positioning point variations can be obtained with a concrete function expression.

Propagation model of variation resulted from assembly deformation

Assembly variation indicates the offset that a part's actual assembled position deviates from designed assembly specification or its nominal position required in each assembly process. And the variations of the point on axis x_1 of the stringer due to positioning variation is denoted by

$$\Delta u_i(x_1)=u_i(x_1)-{}^0u_i(x_1)(i=1,2,3), \tag{35}$$

where $u_i(x_1)$ $(i=1,2,3)$ are coordinate values for the actual positions of the points on axis x_1 of the positioned stringer, ${}^0u_i(x_1)$ $(i=1,2,3)$ are coordinate values for their nominal positions, thus we have ${}^0u_i(x_1)=0$ $(i=1,2,3)$.

[insert Figure 6.]

When the stringer is discretized, as shown in Fig. 6, coordinate system $\{{}^0O\}$ represents the nominal position of stringer while coordinate system $\{O\}$ represents the actual position of assembled stringer. Point ${}^0O$ is the centre of inertia of the cross-section and the principal directions of coordinate system $\{{}^0O\}$ as ${}^0X_1$, ${}^0X_2$ and ${}^0X_3$, parallel to the axes x_1, x_2 and x_3 as known. When written in terms of coordinate system $\{O\}$, they are called X_1, X_2 and X_3. The displacement of any point ${}^0P$ on the cross-section of stringer is described by vector with respect to system $\{{}^0O\}$, which can be calculated by

$$\begin{aligned}
\overrightarrow{{}^0\mathbf{PP}} &= \overrightarrow{{}^0\mathbf{OP}} - \overrightarrow{{}^0\mathbf{O}\,{}^0\mathbf{P}} \\
&= {}^0\mathbf{R}\cdot\overrightarrow{\mathbf{OP}} + \overrightarrow{{}^0\mathbf{OO}} - \overrightarrow{{}^0\mathbf{O}\,{}^0\mathbf{P}} \\
&= {}^0\mathbf{R}\cdot\overrightarrow{{}^0\mathbf{O}\,{}^0\mathbf{P}} - \overrightarrow{{}^0\mathbf{O}\,{}^0\mathbf{P}} + \overrightarrow{{}^0\mathbf{OO}} \\
&= \left({}^0\mathbf{R}-\mathbf{E}\right)\cdot\left[\begin{array}{ccc} {}^0x_1^P-{}^0x_1^O & {}^0x_2^P-{}^0x_2^O & {}^0x_3^P-{}^0x_3^O \end{array}\right]^T + \mathbf{\Delta u_i} \\
&= \left({}^0\mathbf{R}-\mathbf{E}\right)\cdot\left[\begin{array}{ccc} {}^0x_1^P & {}^0x_2^P & {}^0x_3^P \end{array}\right]^T + \left[\begin{array}{ccc} \Delta u_1 & \Delta u_2 & \Delta u_3 \end{array}\right]^T,
\end{aligned} \tag{36}$$

where the rotation matrix describes $\{O\}$ relative to $\{{}^0O\}$

$${}^0\mathbf{R}(\omega_1,\omega_2,\omega_3)=\begin{bmatrix} c\omega_3\cdot c\omega_2 & c\omega_3\cdot s\omega_2\cdot s\omega_1 - s\omega_3\cdot c\omega_1 & c\omega_3\cdot s\omega_2\cdot c\omega_1 + s\omega_3\cdot s\omega_1 \\ s\omega_3\cdot c\omega_2 & s\omega_3\cdot s\omega_2\cdot s\omega_1 + c\omega_3\cdot c\omega_1 & s\omega_3\cdot s\omega_2\cdot c\omega_1 - c\omega_3\cdot s\omega_1 \\ -s\omega_2 & c\omega_2\cdot s\omega_1 & c\omega_2\cdot c\omega_1 \end{bmatrix}, \tag{37}$$

where $c\omega_i = \cos\omega_i, s\omega_i = \sin\omega_i, i = 1,2,3$. Thereby, when the stringer is clamped and positioned, a model for propagating variation of point ${}^0O$ (the centre of inertia of the cross-section) to variation of point ${}^0P$ (any point on the same cross-section of stringer) is given by

$$\mathbf{\Delta u_i^P} = \left({}^{\mathbf{0}}\mathbf{R} - \mathbf{E}\right)\cdot\left[{}^0x_1^P \quad {}^0x_2^P \quad {}^0x_3^P\right]^T + \mathbf{\Delta u_i^0}, (i = 1,2,3), \tag{38}$$

where $\left[{}^0x_1^P \quad {}^0x_2^P \quad {}^0x_3^P\right]^T$ is the position vector of point ${}^0P$ with respect to system $\{{}^0O\}$.

Case study of stringer positioning deformation and finite element simulation

Case study: Theoretical calculation of stringer positioning deformation

The angle between the direction of gravity and the normal direction of the locating surface for the stringer, θ, is shown in Fig. 7. Fig. 8 shows the sectional dimension of the stringer. Other parameters of the stringers are presented in Table 1 and Table 2.

[insert Figure 7.]

[insert Figure 8.]

Table 1 Boundary conditions of theoretical model

Variable	x_1/mm	$u_1(x_1)$/ mm	$\omega_1(x_1)$/rad	$u_2(x_1)$/mm	$\omega_2(x_1)$/rad	$u_3(x_1)$/mm	$\omega_3(x_1)$/rad

δ_1	10	0	0	0	0	0	0
δ_2	485	0.458	-0.0897	-1.856	0	-2.439	-0.0437

Table 2 Physical and mechanical property parameters of the materials

Part	Material	Density ρ (g·cm^{-3})	Cross-sectional area A (mm^2)	Young modulus E (GPa)	Poisson's ratio v
Stringer	7050-T7651	2.83	166.5	72	0.33

The parameters are substituted into the equilibrium equations Eq. (31), we have

$$10 < x_1 < 485: \begin{cases} -EAu_1'' = f_1 \\ -EI_{32}u_3^{(4)} + EI_{33}u_2^{(4)} = f_2 \\ EI_{22}u_3^{(4)} - EI_{23}u_2^{(4)} = f_3 \\ -\dfrac{E}{2(1+v)} J\omega_1'' = m_1 \end{cases},$$

where $I_{32}=I_{23}=1.403\times10^4 mm^4$, $I_{33}=2.342\times10^4 mm^4$, $I_{22}=1.427\times10^4 mm^4$ which are calculated, based on the sectional dimension of the stringer shown in Fig.8. The result of equations is $u_2^{(4)} = constant, u_3^{(4)} = constant$, thus the displacements are assumed to be given by $u_i = a_i x_1^4 + b_i x_1^3 + c_i x_1^2 + d_i x_1 + e_i, i = 2,3$. Similar to the case of the other displacement and rotation, they are expressed by $u_i = d_i x_1 + e_i, i = 1,4$, in terms of their constant second derivative which is 0, namely $u_1^{(2)}=0, u_4^{(2)}=0$. Values of coefficients of the function expressions are calculated and shown in Table 3.

Table 3 Calculated values of coefficients of the function expressions

Coefficient	a_i	b_i	c_i	d_i	e_i
i=1				9.641×10^{-4}	-9.641×10^{-3}
i=2	-3.477×10^{-13}	-1.588×10^{-7}	7.205×10^{-5}	-1.393×10^{-3}	6.8875×10^{-3}
i=3	-5.189×10^{-13}	4.603×10^{-8}	-3.393×10^{-5}	6.6476×10^{-4}	-3.301×10^{-3}
i=4				-1.8884×10^{-4}	1.8884×10^{-3}

Finite element simulation

FE model of a lateral fuselage panel component stringer is created using ABAQUS® CAE as the pre-processor. The FE analysis (FEA) is carried out using the general-purpose FEA package ABAQUS® Standard. Solid elements are generally adapted to model. Since the obtained result of displacement cannot directly show the rotation of stringer deformation with torsion is applied, so beam elements are required for stringer modeling to obtain rotation displacements at each point of stringer around the axis x_1. B31 elements are adopted to mesh the grids of stringer. The material parameters are shown in Table 2. Applied displacement boundary conditions are presented in Table 1 and gravity is also concerned in the model. FE results of beam deformation caused by variations of positioning point and gravity are shown in Fig. 9.

[insert Figure 9.]

Comparisons between results from the proposed theoretical model calculation and Abaqus® simulation are demonstrated in Fig.10. It is clear that they are consistent and have the same accuracy.

[insert Figure 10.]

Experiment

The stringer is positioned with a dedicated fixture for positioning and clamping, with a distance of 475 mm between the two clamping elements, as is illustrated in Fig. 2. Leica AT901-LR® laser tracker is adopted to measure the surface of the stringer deformation arising in assembly. Displacements of all points and positions measured in the experiments are shown in Fig. 11. The edge reflector holder and the shankless reflector holder are respectively allocated on the edge and the offset line of the edge to measure the coordinate values of all points.

[insert Figure 11.]

Constraint displacements of Δu_1, Δu_2, Δu_3 and rotation angles of $\Delta\omega_1$, $\Delta\omega_2$, $\Delta\omega_3$ are applied on the clamped location by adding shims between clamping element rectangular block 2 and stringer surface. As shown in Fig. 12, rotation angle ω is calculated by

$$\omega=\arctan\left(\frac{d}{l}\right), \tag{39}$$

[insert Figure 12.]

Constraints of displacements and rotation angles adopted in the experiments are listed in Table 4.

Table 4 Input values of variations in single and multi-factor experiments

Constraints	Δu_1/mm	Δu_2/mm	Δu_3/mm	$\Delta\omega_1$/rad	$\Delta\omega_2$/rad	$\Delta\omega_3$/rad
I	0	0	-1.68	0	0	0
II	0	-2	0	0	0	0
III	0	2	0	0	0	0
IV	0.195	-0.952	0	0	0	-0.0187
V	0.458	-1.856	-2.439	-0.0897	0	-0.0437

Applications of boundary conditions in the experiments are shown in Fig. 13

[insert Figure 13.]

As a benchmark, the nominal coordinate system of the stringer serves as an initial position in the actual coordinate system, and since this paper takes no account of manufacturing errors, we have ${}^0u_i(x_1)=0 \quad (i=1,2,3)$. Variation values of the centeral axis of inertia of the stringer cross-section are displacement values of their deformation. With the use of the model, which propagates variations of the centeral axis of inertia of the cross-sections to the variations of all points on the stringer, theoretical variation values of

points on the stringer is available. Comparisons between measured values of u_1, u_2, u_3 (actual variations) on the offset lines of bb_1, cc_1, dd_1 and calculated theoretical variation values are made as shown in Fig. 14.

[insert Figure 14.]

From u_2, u_3, the actual values of dd_1's variations on the direction of x_2, x_3, as shown in (a), (b), (c), (d) in Fig. 14, it can be seen that u_2, x_2-direction deformations of each point on the stringer, are exclusively determined by Δx_2 and $\Delta\omega_3$, uncorrelated with deformations on the other two coordinate directions. In the statistical analysis of actually-measured values of dd_1 in multi-factor experiment V, as seen in Table 5, the result Sig.>0.1 indicates u_2 and u_3 are uncorrelated. Therefore, basic hypotheses of the proposed method about 'deformation prediction model for stringer positioning assembly' presented in Section 2.1, has been proven consistent with practice. Because of the random error occurs in the experiment process, a few actually-measured data deviate from theoretical values which are zero as shown in Fig. 14. According to means and standard deviations of the variations between experimental and theoretical values of dd_1, as is listed in Table 6, combining with the simulation result in Section 3.2, it can be concluded theoretical variation model is consistent with simulation result, conforming to the tendency of experimental values and applicable to engineering purpose. It can also be

derived that theoretical result calculated by variation propagation model is consistent with actual measurement from comparison among actually-measured values on multiple positions of bb_1, cc_1, dd_1.

Table 5 Statistical analysis results for experiment V

		u_2	u_3
u_2	Pearson Correlation	1	.296
	Sig. (2-tailed)		.377
	N	11	11
u_3	Pearson Correlation	.296	1
	Sig. (2-tailed)	.377	
	N	11	11

Table 6 Means and standard deviations of the variations between experimental and theoretical values of dd1 in the experiment

Conditions	Means of variations/mm		Standard deviations of variations/mm	
	$\overline{\delta_{u_2}}$	$\overline{\delta_{u_3}}$	σ_{u_2}	σ_{u_3}
I	0.0549065	0.1118076	0.136257	0.147843
II	0.014618	-0.08415	0.16724	0.125298
III	0.234211	0.099978	0.252261	0.153608
IV	-0.215753	0.095336	0.181135	0.085481
V	-0.355435	0.282771	0.380336	0.206827

Conclusions

Dimensional variation caused by deformation of the large component is a major problem that aircraft industry is faced with. To solve deformation problems in assembly caused by positioning variation, based on elasticity theory of the principle of minimum potential energy and spatial transformations of coordinate, this paper presented a theoretical model for predicting deformation of compliant part and a variation propagation model for determining the relationship between local variations and the whole assembly variations. Main conclusions are as follow:

(1) The stringer has been simplified into an elastic beam, as the cross-section width is much smaller than the length. Based on energy conservation theory, deformation potential of the stringer caused by variation of positioning point can be calculated by stacking up strain energies separately caused by tension, bending moment, torque and shear force applying on the stringer. The deformation potential has been minimized to get a function expression of displacement and rotation angle of each part of deformed complaint component. Thus, a non-linear relationship between positioning point variation and assembly deformation has been obtained, and the basic hypotheses moderately conform to practice.

(2) FE model of panel component was created using ABAQUS® CAE commercial software. Beam elements B31 has been adopted to divide finite element model and deformation arising in positioning and clamping operation are simulated. FE simulation analysis results of assembly deformation of stringer parts were consistent with the calculated results of proposed theoretical model experimental results, which verified the accuracy of theoretical model.

(3) Leica AT901-LR® laser tracker has been used for measuring the point coordinates on the surface of the deformed stringer after positioning and clamping process. Therefore, the variations of position coordinates of the points are approachable, which can be compared with results of the theoretical model. It has been proven that variation propagation model is correct and the proposed method satisfies the project application.

The study of stringer's assembly deformation caused by variation arising in the positioning and clamping process is a preliminary to panel assembly variation research. To meet with design requirement, variations present in the joining assembly of panel components including stringer, frame and skin need further investigation. Calculation results derived from the proposed theoretical model for predicting stringer deformation can be used as input conditions in the subsequent study of panel assembly variation and

can also provide a basis for error sources investigation and mechanism study on how the assembly technology influents the assembly quality.

Declaration of conflicting interests

The authors declare that there is no conflict of interest.

Funding

This work was supported by the National Natural Science Foundation of China [grant number 51375442].

References

1. Chang MH and Gossard DC. Modeling the assembly of compliant, non-ideal parts. Comput Aided Design. 1997; 29: 701-708.

2. Liu SC and Hu SJ. An offset finite-element model and its applications in predicting sheet-metal assembly variation. Int J Mach Tool Manu. 1995; 35: 1545-1557.

3. Liu SC, Hu SJ and Woo TC. Tolerance analysis for sheet metal assemblies. J Mech Des-T ASME. 1996; 118: 62-67.

4. Dahlstrom S and Soderberg R. Towards a method for early evaluations of sheet metal assemblies. In: Bourdet P and Mathieu L (eds) *Geometric product specification and verification: integration of functionality*. Dordrecht: Springer, 2003, pp.275-286.

5. Cai WW, Hsieh CC, Long YF, and et al. Digital panel assembly methodologies and applications for compliant sheet components. J Manuf Sci E-T ASME. 2006; 128: 270-279.

6. Vichare P, Martin O and Jamshidi J. Dimensional management for aerospace assemblies: framework implementation with case-based scenarios for simulation and measurement of in-process assembly variations. Int J Adv Manuf Tech. 2014; 70: 215-225.

7. Lin J, Jin S, Zheng C, Li ZM and et al. Compliant assembly variation analysis of aeronautical panels using unified substructures with consideration of identical parts. Comput Aided Design. 2014; 57: 29-40.

8. Liu SC and Hu SJ. Variation simulation for deformable sheet metal assemblies using finite element methods. J Manuf Sci E-T ASME. 1997; 119: 368-374.

9. Camelio JA, Hu SJ and Marin SP. Compliant assembly variation analysis using component geometric covariance. J Manuf Sci E-T ASME. 2004; 126: 355-360.

10. Liao XY and Wang GG. Wavelets-based method for variation analysis of non-rigid assemblies. Int J Mach Tool Manu. 2005; 45: 1551-1559.

11. Karmakar S and Maiti J. A review on dimensional tolerance synthesis: paradigm shift from product to process. Assembly Autom. 2012; 32: 373-388.

12. Bowman RA. Efficient gradient-based tolerance optimization using monte carlo simulation. J Manuf Sci E-T ASME. 2009; 131: 337-346.

13. Wang H. Deformation Deformation analysis in horizontal stabilizer assembly using FEA modeling and multilevel analysis. J Aerospace Eng. Epub ahead of print 28 Mar 2015. DOI: 10.1061/(asce)as.1943-5525.0000385.

14. Abedini V, Shakeri M, Siahmargouei MH and et al. Analysis of the influence of machining fixture layout on the workpiece's dimensional accuracy using genetic algorithm. Proc IMechE Part B: J Engineering Manufacture. 2014; 228: 1409-1418.

15. Liu P, Li Y, Zhang KF and Cheng H. Based on region division setup planning for sheet metal assembly in aviation industry. Proc IMechE Part B: J Engineering Manufacture. 2013; 227: 153-161.

16. Ding Y, Shi JJ and Ceglarek D. Diagnosability analysis of multi-station manufacturing processes. J Dyn Syst-T ASME. 2002; 124: 1-13.

17. Liu CH, Jin S, Lai XM and et al. Dimensional variation stream modeling of investment casting process based on state space method. Proc IMechE Part B: J Engineering Manufacture. 2015; 229: 463-474.

18. Ceglarek D and Prakash PKS. Enhanced piecewise least squares approach for diagnosis of ill-conditioned multistation assembly with compliant parts. Proc IMechE Part B: J Engineering Manufacture. 2012; 226: 485-502.

19. Xie K. *Analysis, prediction and control of variation propagation in non-linear sheet metal assembly processes*. PhD Thesis, Michigan Technological University, USA, 2009.

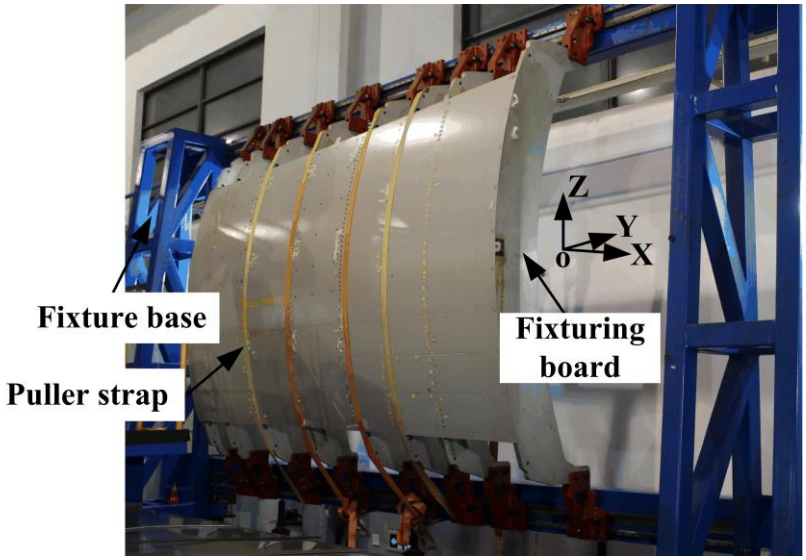

Figure 1. Panel assembly fixture

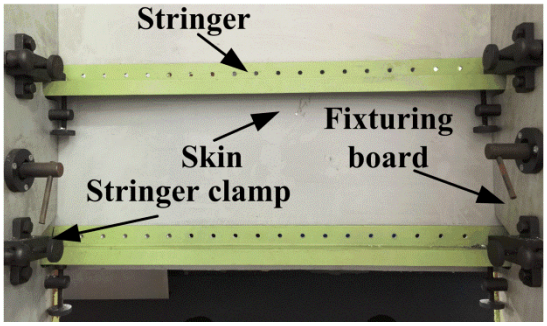

Figure 2. Stringer positioning element

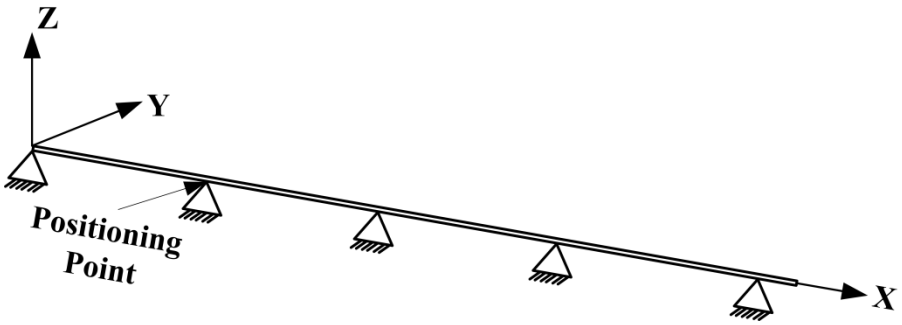

(a) Nominal position of a stringer

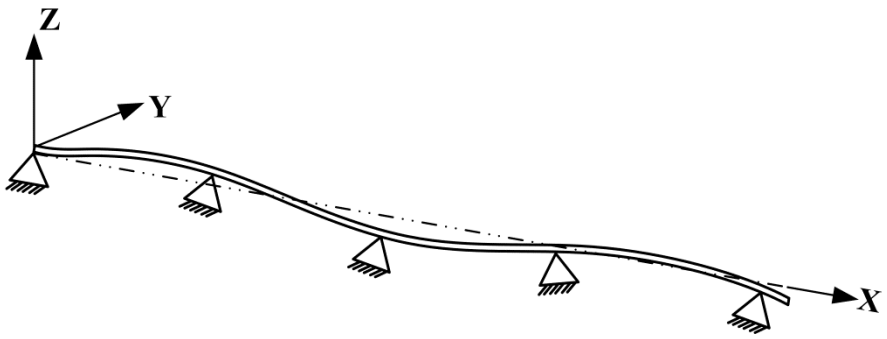

(b) Positioning point variations and stringer deformation

Figure 3. Mechanical simplification of the stringer and positioning element

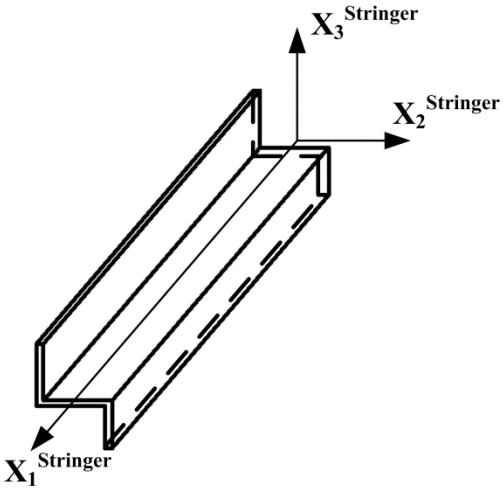

Figure 4. Local coordinate system

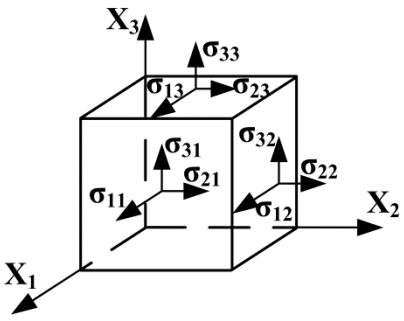

Figure 5. Directions of stress component

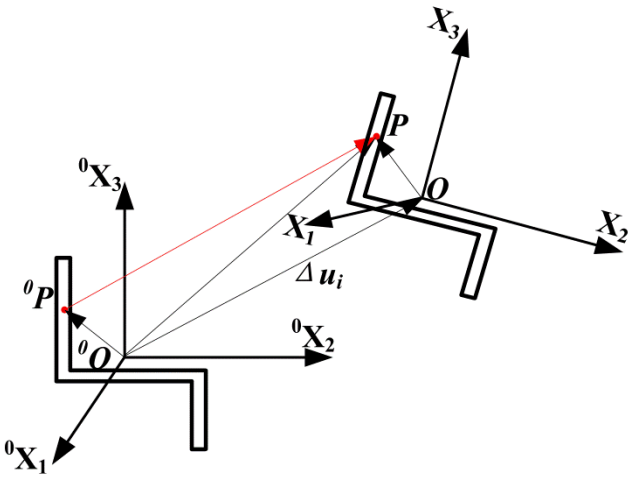

Figure 6. Coordinate transformation of position points on the same cross-section of stringer

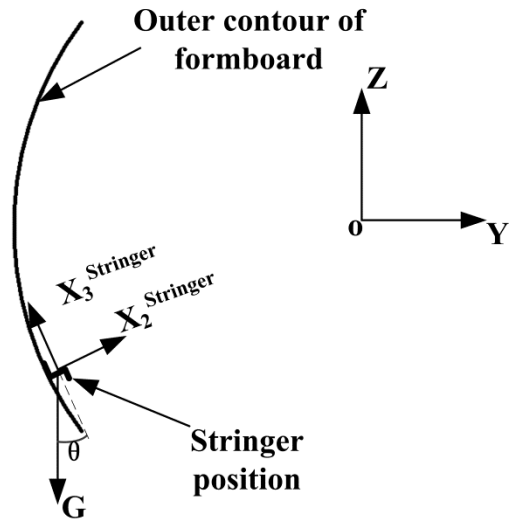

Figure 7. Position and direction of stringer in assembly process

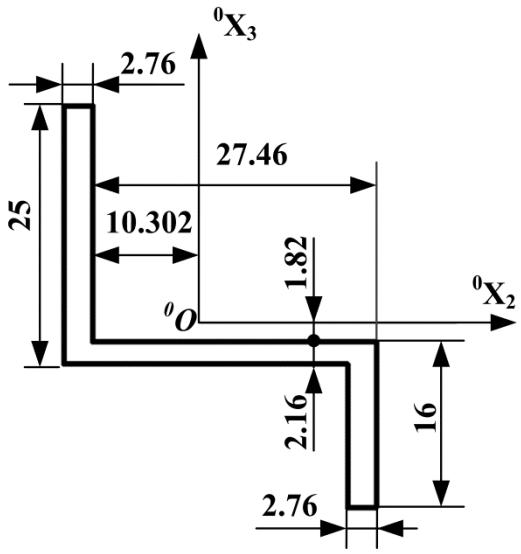

Figure 8. Sectional dimension of the stringer

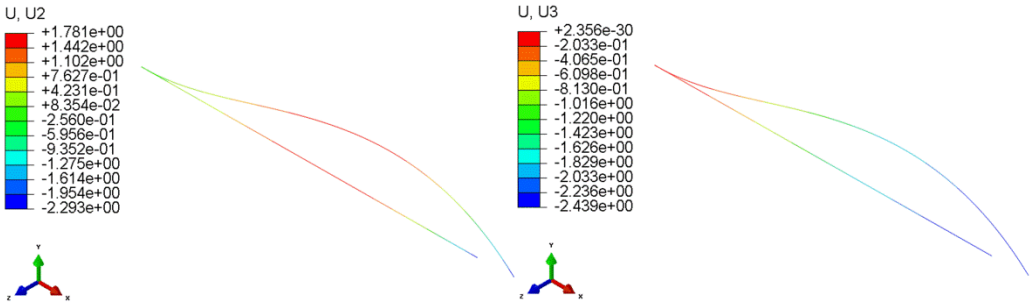

Figure 9. FE results of beam deformation

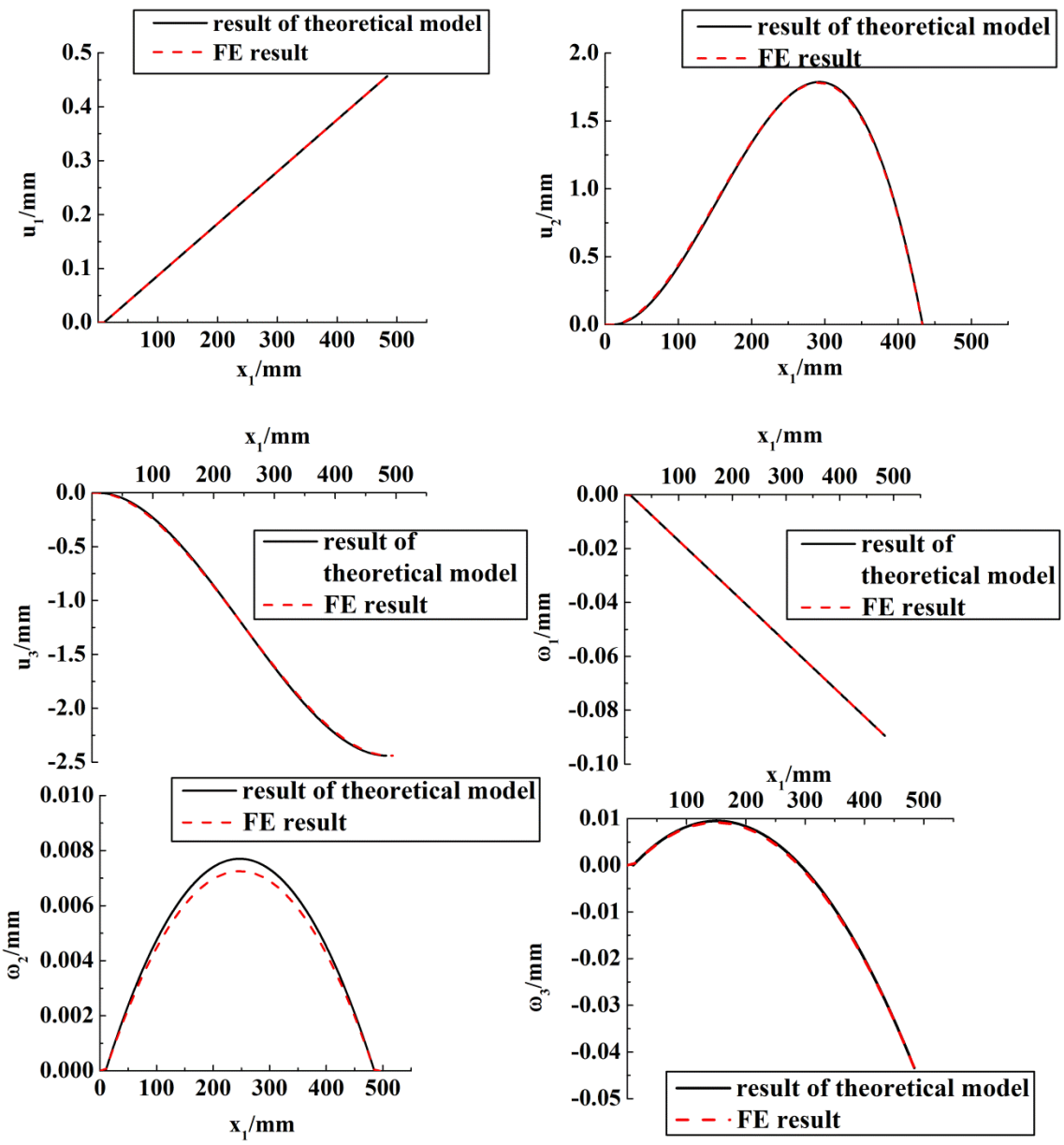

Figure 10. Comparison between results from theoretical model calculation and Abaqus® simulation

Figure 11. The location of surface points of stringer to be measured

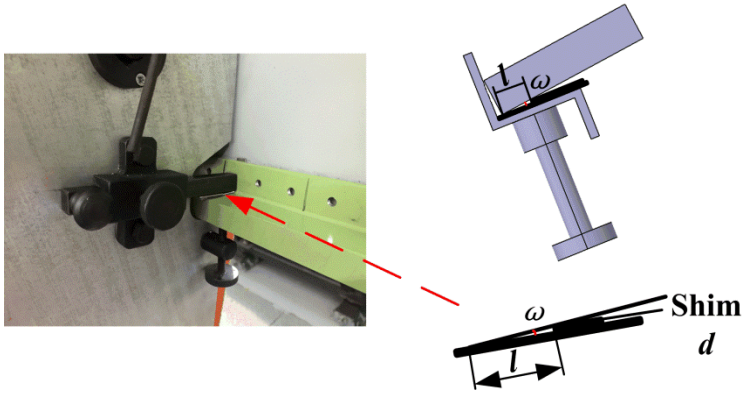

Figure 12. Methods and rotation angles applied to create variations in stringer assembly

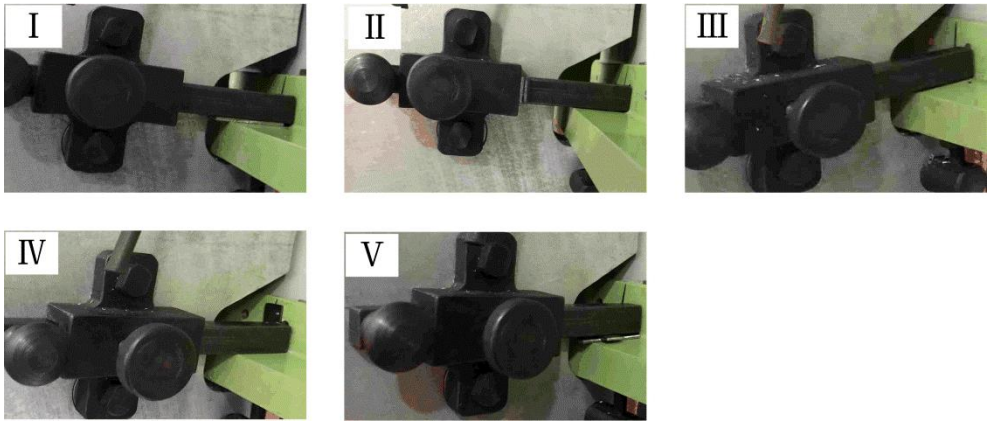

Figure 13. Applications of boundary conditions in the experiments

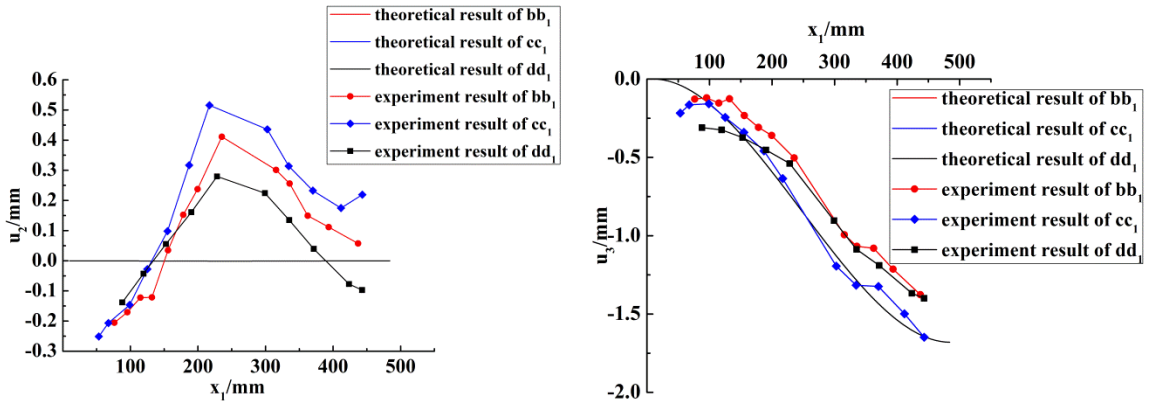

(a) Theoretical and measured values of the position variations of bb_1, cc_1, dd_1 with the change of x_1 on the direction of x_2, x_3 in experiment I

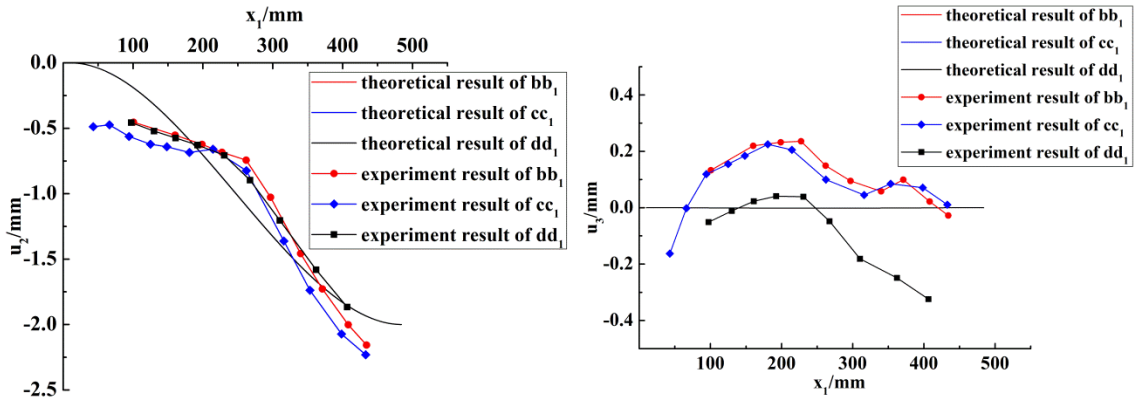

(b) Theoretical and measured values of the position variations of bb_1, cc_1, dd_1 with the change of x_1 on the direction of x_2, x_3 in experiment II

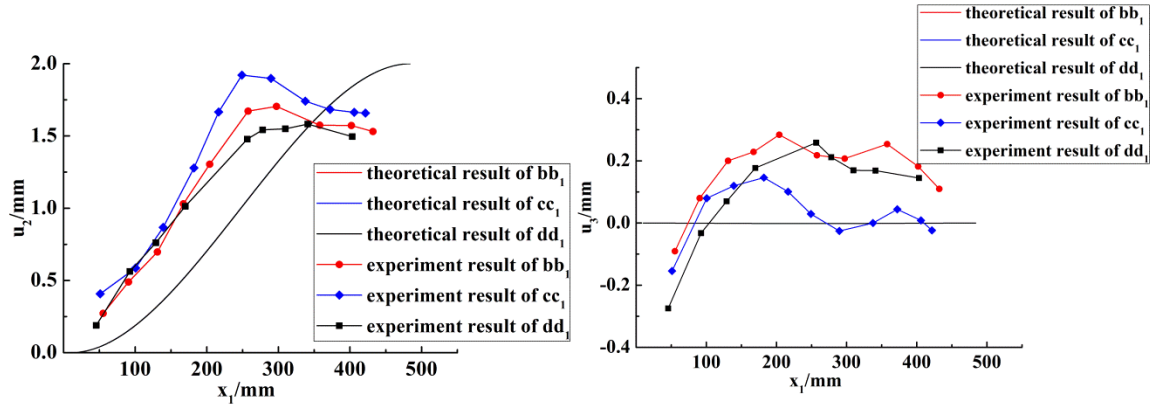

(c) Theoretical and measured values of the position variations of bb_1, cc_1, dd_1 with the change of x_1 on the direction of x_2, x_3 in experiment III

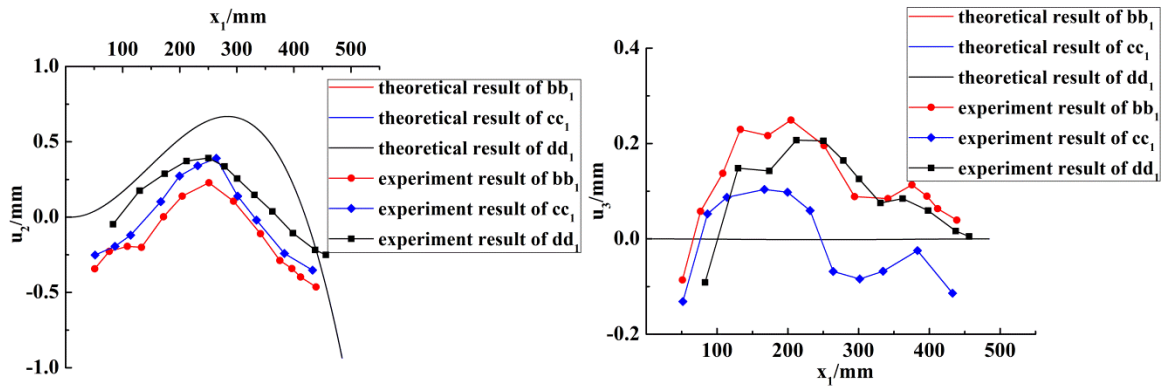

(d) Theoretical and measured values of the position variations of bb_1, cc_1, dd_1 with the change of x_1 on the direction of x_2, x_3 in experiment IV

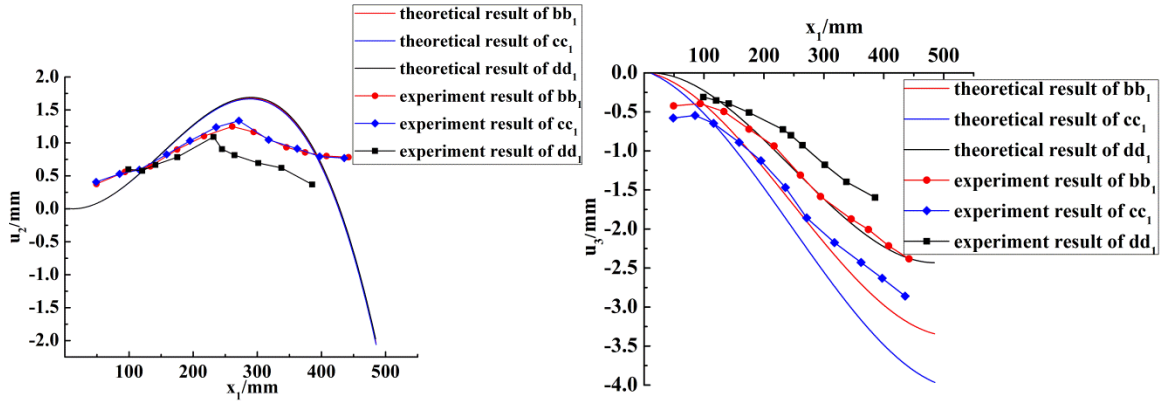

(e) Theoretical and measured values of the position variations of bb_1, cc_1, dd_1 with the change of x_1 on the direction of x_2, x_3 in experiment V

Figure 14. Calculated theoretical variation values and measured values (actual variations) of the offset lines bb_1, cc_1, dd_1